NRC Research Press

ARTICLE

Synthesis, structure, and properties of the hexagermane $Pr^i_3Ge(GePh_2)_4GePr^i_3$

Kimberly D. Roewe, James A. Golen, Arnold L. Rheingold, and Charles S. Weinert

Abstract: The synthesis of the hexagermane $Pr^i_3Ge(GePh_2)_4GePr^i_3$ was achieved starting from the cyclotetragermane $(Ph_2Ge)_4$. Ring-opening of $(Ph_2Ge)_4$ with Br_2 yielded $Br(GePh_2)_4Br$ that was converted to $H(GePh_2)_4H$, and this material was treated with two equiv. of $Pr^i_3GeNMe_2$ to furnish $Pr^i_3Ge(GePh_2)_4GePr^i_3$ via the hydrogermolysis reaction. The X-ray crystal structures of $(Ph_2Ge)_4$, $Br(GePh_2)_4Br$ and $Pr^i_3Ge(GePh_2)_4GePr^i_3$ were determined. The hexagermane $Pr^i_3Ge(GePh_2)_4GePr^i_3$ represents the longest structurally characterized linear oligogermane reported to date and exhibits physical properties that resemble those of the larger polygermane systems. The hexagermane is luminescent and interacts with polarized light, appearing pale yellow under one orientation of polarized light and deep blue under the opposite orientation. The electrochemistry of $Pr^i_3Ge(GePh_2)_4GePr^i_3$ was also explored, and this species exhibits the expected five irreversible oxidation waves.

Key words: germanium, main group chemistry, luminescence, X-ray crystal structure, electrochemistry.

Résumé : La synthèse de l'hexagermane $Pr^i_3Ge(GePh_2)_4GePr^i_3$ a été réalisée à partir d'un cyclotetragermane $(Ph_2Ge)_4$. L'ouverture du cycle de $(Ph_2Ge)_4$ en présence de Br_2 a donné la molécule $Br(GePh_2)_4Br$, qui a été convertie en $H(GePh_2)_4H$. Celle-ci est mise en présence de deux espèces de formule $Pr^i_3GeNMe_2$ de façon à produire le composé $Pr^i_3Ge(GePh_2)_4GePr^i_3$ par hydrogermolyse. On a ensuite déterminé les structures cristallines de $(Ph_2Ge)_4$, $Br(GePh_2)_4Br$ et de $Pr^i_3Ge(GePh_2)_4GePr^i_3$, obtenues par cristallographie aux rayons X. L'hexagermane de formule $Pr^i_3Ge(GePh_2)_4GePr^i_3$ constitue l'oligogermane possédant la plus longue structure linéaire caractérisée à ce jour et présente des propriétés physiques ressemblant à celles des polygermanes de plus grande taille. L'hexagermane est luminescent et interagit avec la lumière polarisée, apparaissant en jaune pâle sous une lumière polarisée dans une certaine direction et en bleu foncé sous une lumière polarisée dans la direction opposée. L'analyse électrochimique du composé $Pr^i_3Ge(GePh_2)_4GePr^i_3$ permet de confirmer que ce dernier présente les cinq vagues d'oxydation auxquelles on s'attendait. [Traduit par la Rédaction]

Mots-clés : germanium, chimie des groupes principaux, luminescence, cristallographie cristallographie aux rayons X, électrochimie.

Introduction

Catenated compounds of the Group 14 elements are of significant interest due to their inherent σ-delocalization, which occurs though the overlap of the sp^3 orbitals on each individual atom when these atoms are disposed in a trans-coplanar configuration.[1,2] A number of polymeric Group 14 catenates have been prepared and characterized, but the exact composition of these species are unknown. However, it has been postulated that multiple regions of trans-coplanar atoms are present in these molecules that are terminated by a strong out-of-plane twist. Thus, these molecules can be described as having regions of order that are interrupted by regions of disorder. Of these systems, those containing silicon[2–12] or tin[13–21] have been the most extensively studied, but only a few reports of germanium-containing polymers[22–29] have appeared.

An effective method for the preparation of polygermanes involves the demethanative coupling of germanes, having the general formula RR'GeMeH, using a ruthenium-based catalyst,[22–25,29] and other preparative routes including the electropolymerization of germanium halides[26,28] have also been described. Polygermanes, examples of which are $[(p\text{-}(MeO)_3SiC_6H_4)MeGe]_n$,[22] $H(GeMe_2)_nMe$,[25] $H(GeMeAr)_nMe$ (Ar = Ph, *p*-Tol, *p*-FC_6H_4, *p*-$F_3CC_6H_4$, *m*-$Me_2C_6H_3$, *p*-$(H_3CO)C_6H_4$),[23] $(R_2Ge)_n$, (R = Me. Bu^n, or Ph),[27] and *m*-(*S*)-2-methylbutylphenyldimethylpolygermane,[29] have a number of interesting and potentially useful properties, including fluorescence and conductivity. These properties might result in germanium-based polymers being used as new materials, especially as the limitations of silicon-based materials begin to be realized.

Oligogermanes, which are discrete compounds that have defined compositions and structures, can function as small-molecule models for the larger polygermane systems.[30–34] In addition, these molecules are expected to exhibit physical properties similar to those of the polygermanes, provided a sufficient number of catenated germanium atoms can be obtained. We have postulated for some time that long-chain oligogermanes would behave in this fashion, since the polygermanes can be regarded as having several arrays of trans-coplanar germanium atoms. A few of these types of compounds are known, including the long-chain methyl substituted oligogermanes Ge_6Me_{14}[35] and $Ge_{10}Me_{22}$.[36] However, these two oligogermanes have not been fully characterized, and the pentagermane Ge_5Ph_{12} represents the longest structurally characterized oligogermane that has been reported to date.[37,38] We have re-

Received 24 October 2013. Accepted 20 January 2014.

K.D. Roewe and C.S. Weinert. Department of Chemistry, Oklahoma State University, Stillwater, OK 74078, USA.
J.A. Golen. Department of Chemistry and Biochemistry, University of Massachusetts Dartmouth, North Dartmouth, MA 02747, USA; Department of Chemistry and Biochemistry, University of California San Diego, La Jolla, CA 92093-0358, USA.
A.L. Rheingold. Department of Chemistry and Biochemistry, University of California San Diego, La Jolla, CA 92093-0358, USA.
Corresponding author: Charles S. Weinert (e-mail: weinert@chem.okstate.edu).

This article is part of a Special Issue commemorating the 14th International Conference on the Coordination and Organometallic Chemistry of Germanium, Tin, and Lead (ICCOC-GTL 2013) held in Baddeck, NS, July 2013.

Scheme 1.

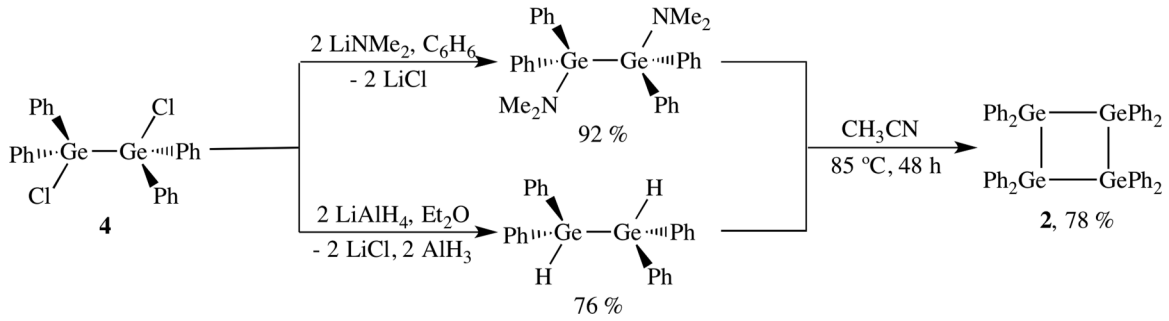

cently prepared Ge_5Ph_{12} via the hydrogermolysis reaction and did not observe any luminescent behavior or unusual optical properties for this compound; rather, Ge_5Ph_{12} was a colorless solid with a UV–vis absorbance maximum at 295 nm.[37,38]

Over the past several years we have employed the hydrogermolysis reaction for the formation of single germanium–germanium bonds.[30,32,33,38–49] This method employs a germanium amide R_3GeNMe_2 and a germanium hydride R'_3GeH as starting materials and proceeds in acetonitrile solvent. The CH_3CN solvent acts not only as a reaction medium but also as a reagent, as we have shown that the amide R_3GeNMe_2 is converted in situ to the α-germyl nitrile R_3GeCH_2CN, and it is this species that is the active reagent in the Ge–Ge bond forming process.[39,50] Using this methodology, we have prepared an array of linear and branched oligogermanes that have been characterized using NMR (^1H, ^{13}C, ^{73}Ge[43,45,46,51]) spectroscopy, elemental analysis, and in many cases X-ray crystallography. We have endeavored to prepare linear systems having more than five catenated germanium atoms, with the expectation that some of these long-chain systems would have physical properties that would mirror those of the polymeric systems. We have recently prepared the hexagermane $Pr^i_3Ge(GePh_2)_4GePr^i_3$ (**1**) in three steps starting from the cyclotetragermane $(GePh_2)_4$ (**2**), where the final step involves attachment of two germanium atoms to the hydride-terminated tetragermane $H(GePh_2)_4H$ (**3**) via the hydrogermolysis reaction.[52,53] The hexagermane **1** has been shown to be luminsescent in CH_2Cl_2 solution and also displays dramatic dichroic behavior when observed under opposite directions of polarized light. The detailed synthesis of **1**, as well as an investigation of its physical properties, are the foci of this article.

Results and discussion

The synthesis of the cyclotetragermane $(GePh_2)_4$ (**2**) was reported in 1986 and was prepared via treatment of Ph_2GeCl_2 with sodium metal in refluxing toluene.[54] Although this is a reliable preparative route for **2**, the reported yield was only 33%. We have recently obtained **2** via a different route that illustrates that the hydrogermolysis reaction can be used for the preparation of cyclic oligogermanes in addition to the branched and linear systems (Scheme 1). The preparation of the 1,2-dichlorodigermane $ClPh_2GeGePh_2Cl$ (**4**) was carried out via the literature procedure,[42,55] and we have for the first time obtained the X-ray crystal structure of this material.

An ORTEP diagram of **4** is shown in Fig. 1 and selected bond distances and angles are collected in Table 1. Compound **4** crystallizes with two independent molecules in the unit cell, and both of these lie on a two-fold axis of rotation. Molecule 1 is completely ordered, while molecule 2 is a composite of two orientations having Ge(2) and Cl(2) disordered over two positions with relative occupancies of 50% in each case. The bond lengths listed in Table 1 for molecule 2 of **4** are an average of these two orientations. The average Ge–Ge bond distance in **4** in the two molecules is 2.394(2) Å, which is shorter than the Ge–Ge bond distance in $Ge_2Ph_6{\bullet}C_6H_6$ that measures 2.446(1) Å,[56] and this is due to the

Fig. 1. ORTEP diagram of $ClPh_2GeGePh_2Cl$ (**4**). Thermal ellipsoids are drawn at 50% probability.

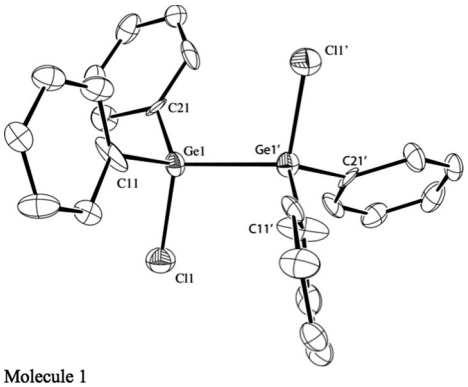

Molecule 1

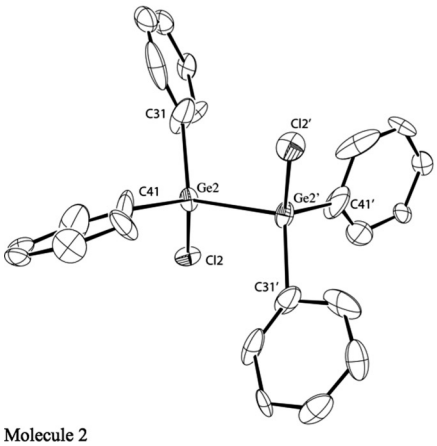

Molecule 2

Table 1. Selected bond distances (Å) and angles (°) for $ClPh_2GeGePh_2Cl$ (**4**).

Molecule 1		Molecule 2	
Bond distances (Å)			
Ge(1)–Ge(1′)	2.397(1)	Ge(2)–Ge(2′)	2.391(2)
Ge(1)–Cl(1)	2.182(2)	Ge(2)–Cl(2)	2.178(3)
Ge(1)–C(11)	1.931(6)	Ge(2)–C(31)	2.000(7)
Ge(1)–C(21)	1.879(7)	Ge(2)–C(41)	1.953(8)
Bond angles (°)			
Cl(1)–Ge(1)–C(11)	106.4(2)	Cl(2)–Ge(2)–C(31)	115.4(4)
Cl(1)–Ge(1)–C(21)	107.2(2)	Cl(2)–Ge(2)–C(41)	115.7(3)
C(11)–Ge(1)–C(21)	110.7(3)	C(31)–Ge(2)–C(41)	105.9(3)
Cl(1)–Ge(1)–Ge(1′)	104.67(5)	Cl(2)–Ge(2)–Ge(2′)	103.36(9)
C(11)–Ge(1)–Ge(1′)	110.5(2)	C(31)–Ge(2)–Ge(2′)	106.9(2)
C(21)–Ge(1)–Ge(1′)	116.7(2)	C(41)–Ge(2)–Ge(2′)	109.1(3)

Fig. 2. ORTEP diagram of $(Ph_2Ge)_4$ (**2**). Thermal ellipsoids are drawn at 50% probability.

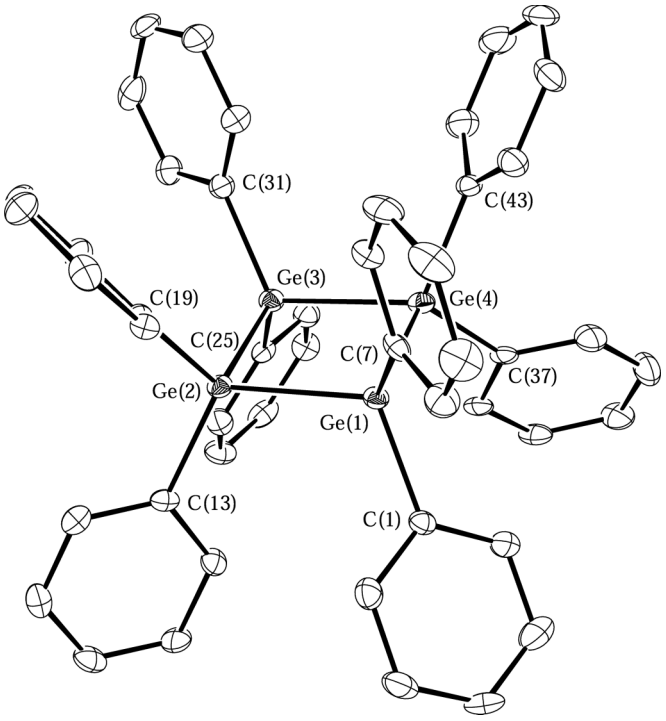

replacement of two phenyl substituents with two chlorine atoms, which are both sterically less encumbering and also more electron-withdrawing.

Compound **4** was converted to both the 1,2-dihydride $HPh_2GeGePh_2H$ and the 1,2-bis(dimethylamido) compound $(Me_2N)Ph_2GeGePh_2(NMe_2)$ via reaction with $LiAlH_4$[42] and $LiNMe_2$, respectively. These two products were then combined in acetonitrile solution in dilute (0.0005 mol/L) conditions to minimize the formation of linear polymeric products, and provided $(GePh_2)_4$ (**2**) in 78% yield. The ^1H and ^{13}C NMR spectra of **2** match those described in the literature.[54] We have obtained a low-temperature (150 K) X-ray structure of **2**, and an ORTEP diagram is shown in Fig. 2, while the metric parameters of **2** are collected in Table 2. The average Ge – Ge bond length in **2** is 2.464(3) Å and the average Ge-Ge-Ge bond angle is 89.95(1)°, which is nearly identical to the expected 90° bond angle, and these parameters are also nearly identical to those reported for the structure that was determined at 22 °C.[54] The related species $(GeTol_2)_4$ (Tol = *p*-$CH_3C_6H_4$)[57] is C_2 symmetric and has an average Ge–Ge bond length and angle of 2.4610(7) Å and 89.02(1)°, respectively. The Ge–Ge distances in the para-tolyl substituted species are slightly shorter than those in **2,** and this has been observed in some other para-tolyl substituted oligogermanes when compared to their phenyl-substituted analogues.[42] The average Ge–Ge bond distances in the cyclotetragermanes $Ge_4Bu^t{}_4Cl_4$ and $Ge_4Pr^i{}_8$ are 2.465(2)[58] and 2.4745(9) Å,[59] respectively, while the average Ge-Ge-Ge bond angles in these species are 89.09(6) and 89.38(2)°. The Ge_4 plane in **2** is puckered by 4.6° and is slightly more distorted than the structure obtained at room temperature that had a ring puckering of 3.9°. The ring puckering in Ge_4Tol_8 is 21.1°, while the corresponding values in the structures of $Ge_4Bu^t{}_4Cl_4$ and $Ge_4Pr^i{}_8$ are 14.6 and 11.9°, respectively. The structure of **2** is less distorted than those of the other three cyclotetragermanes due to the more efficient packing of the phenyl substituents in **2**. The average Ge–Ge bond distance in **2** and $Ge_4Bu^t{}_4Cl_4$ are nearly identical despite the presence of the large tert-butyl groups in $Ge_4Bu^t{}_4Cl_4$, but these four substituents are disposed on opposite sides of the Ge_4 plane in an alternating fashion, which alleviates much of the steric strain.

Table 2. Selected bond distances (Å) and angles (°) for Ge_4Ph_8 (**2**).

Bond distances (Å)	
Ge(1)–Ge(2)	2.4534(4)
Ge(1)–Ge(4)	2.4580(4)
Ge(2)–Ge(3)	2.4730(4)
Ge(3)–Ge(4)	2.4713(4)
Ge(1)–C(1)	1.950(3)
Ge(1)–C(7)	1.952(3)
Ge(2)–C(13)	1.956(3)
Ge(2)–C(19)	1.958(3)
Ge(3)–C(25)	1.956(3)
Ge(3)–C(31)	1.955(3)
Ge(4)–C(37)	1.952(3)
Ge(4)–C(43)	1.958(3)
Bond angles (°)	
Ge(1)–Ge(2)–Ge(3)	90.53(1)
Ge(2)–Ge(3)–Ge(4)	89.03(1)
Ge(3)–Ge(4)–Ge(1)	90.46(1)
Ge(4)–Ge(1)–Ge(2)	89.79(1)
C(1)–Ge(1)–C(7)	107.6(1)
C(13)–Ge(2)–C(19)	110.3(1)
C(25)–Ge(3)–C(31)	106.4(1)
C(37)–Ge(4)–C(43)	105.4(1)
C(1)–Ge(1)–Ge(2)	113.03(8)
C(1)–Ge(1)–Ge(4)	116.46(8)
C(7)–Ge(1)–Ge(2)	113.42(8)
C(7)–Ge(1)–Ge(4)	115.87(8)
C(13)–Ge(2)–Ge(1)	114.56(8)
C(13)–Ge(2)–Ge(3)	115.85(7)
C(19)–Ge(2)–Ge(1)	111.43(8)
C(19)–Ge(2)–Ge(3)	112.90(8)
C(25)–Ge(3)–Ge(2)	118.70(8)
C(25)–Ge(3)–Ge(4)	113.20(8)
C(31)–Ge(3)–Ge(2)	114.71(8)
C(31)–Ge(3)–Ge(4)	114.48(8)
C(37)–Ge(4)–Ge(1)	114.81(7)
C(37)–Ge(4)–Ge(3)	115.64(8)
C(43)–Ge(4)–Ge(1)	116.78(8)
C(43)–Ge(4)–Ge(3)	113.75(8)

The ring-opening of **2** with molecular bromine yields the 1,4-dibromo species $Br(GePh_2)_4Br$ (**5**) in 54% yield (Scheme 2), which is similar to the reported reaction of **2** with I_2 that yielded the 1,4-diiodo substituted analogue $I(GePh_2)_4I$ (**6**).[60] The UV–vis spectrum of **5** has an absorbance maximum at 278 nm that is slightly blue-shifted relative to the reported value for the tetragermane Ge_4Ph_{10} at 282 nm.[61] The difference in the position of λ_{max} for these two species likely stems from the presence of an additional phenyl group at each of the terminal germanium atoms in Ge_4Ph_{12}, as it has been shown that the π-system of the phenyl rings can perturb the energies of the frontier orbitals in these molecules such that the HOMO–LUMO gap in Ge_4Ph_{10} is slightly diminished versus that in **5**.

The X-ray crystal structure of **5** was obtained, and an ORTEP diagram is shown in Fig. 3, while selected bond distances and angles are collected in Table 3. The six heavy atoms in **5** are all disposed in a trans-coplanar arrangement and the average Ge–Ge bond distance in **5** is 2.4473(7) Å. The two Ge–Br bond distances average 2.3540(8) Å, and the average Ge-Ge-Ge and Ge-Ge-Br bonds angles are 113.29(3) and 103.65(3)°, respectively. Each of the germanium atoms in **5** is present in a distorted tetrahedral environment and the Ge–C_{ipso} are all approximately 1.95 Å. The structure of **5** can be compared to the related 1,4-dihalo substituted tetragermanes $I(GePh_2)_4I$ (**6**)[60] and $Cl(GePh_2)_4Cl$ (**7**),[62] both of which have an inversion center along the central Ge–Ge bond that is absent in

Scheme 2.

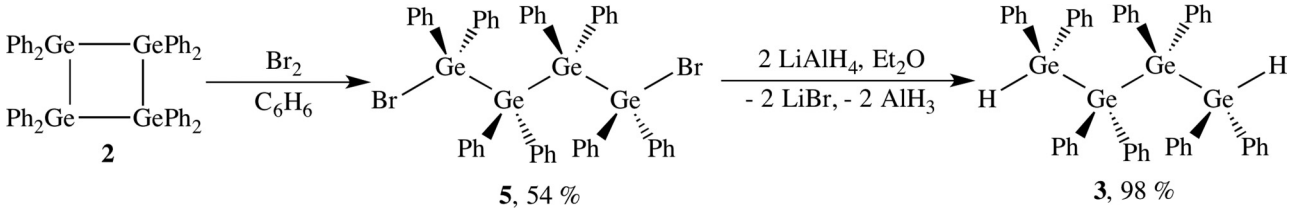

Fig. 3. ORTEP diagram of $Br(GePh_2)_4Br$ (**5**). Thermal ellipsoids are drawn at 50% probability.

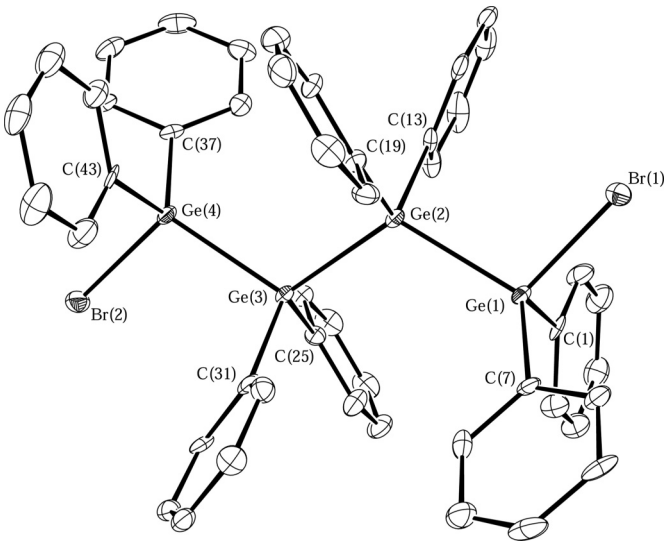

5. The average Ge–Ge bond distances in **6** and **7** are 2.4549(5) and 2.445(3) Å, respectively, and so there is a slight increase in the average Ge–Ge bond distance as the size of the halogen increases. The germanium–halogen distances in **6** and **7** are 2.5594(4) and 2.134(7), respectively, and the germanium–halogen distance in **5–7** therefore increases with the covalent radius of the halogen atom. The unique Ge-Ge-Ge bond angles in **6** and **7** measure 114.2(1) and 116.24(8)°, and the Ge-Ge-X bond angles are 103.4(1) and 100.3(2)°, respectively. The Ge_4X_2 chains in the heavier analogues **5** and **6** are very similar, and that of the chloride-substituted tetragermane **7** differs from those of **5** and **6**.

Compound **5** was converted to the hydrogen-terminated tetragermane $H(GePh_2)_4H$ (**3**) by reaction with $LiAlH_4$ (Scheme 2). We had attempted to convert the iodide-substituted species **6** to **3** under identical conditions but obtained a mixture of **3** combined with several other intractable products. This is likely due to the more highly reducing nature of the iodide anion that may react with the $LiAlH_4$ after the iodine is liberated from the Ge_4 chain. However, **5** could reproducibly be converted to **3** in high yield. The ^1H NMR spectrum of **3** contains a singlet at δ 5.67 ppm arising from the two equivalent germanium-bound protons of **3**, and the infrared spectrum of **3** contains a $\nu_{Ge\text{-}H}$ stretching band at 2000 cm^{-1}. These values correspond well with those reported for **3** that was prepared from Ph_2GeH_2 and Bu^tLi and was identified as a component of a product mixture with $H(GePh_2)_3H$ and $H(GePh_2)_2H$. The λ_{max} for **3** in its UV–vis spectrum was observed at 257 nm, and this is blue shifted compared to the corresponding λ_{max} values for **5** and Ge_4Ph_{10}, since the orbitals of the hydrogen atoms in **3** do not interact with the σ-system of the Ge_4 chain.

A number of oligogermane systems have been characterized using cyclic voltammetry (CV) and differential pulse voltammetry (DPV),[35,38,40,42,45,46,49,52,63] and it has been established that an increase in the degree of catenation in these compounds renders them easier to oxidize and also that the introduction of more highly electron-donating groups at one germanium atom also facilitates the oxidation of the oligogermanes.[49] In addition, we have observed that linear oligogermanes having aryl substituents on at least one germanium atom exhibit $n-1$ successive irreversible oxidation waves, where n is equal to the number of germanium atoms.[38,42,52] However, oligogermanes having halide substituents have not been characterized using these methods, and to our knowledge only one example of a hydride-terminated oligogermane has been studied by CV and DPV.[38]

The CV and DPV of the tetragermane $Br(GePh_2)_4Br$ (**5**) were obtained, and the DPV plot is shown in Fig. 4. Three successive oxidation waves at 1664, 1840, and 2062 mV were observed in the DPV, but these three features were not resolved in the CV of **5**, which is typical for oligogermanes having four our more germanium atoms. A fourth wave was repeatedly observed at ca. 680 mV,

Table 3. Selected bond distances (Å) and angles (°) for $Br(GePh_2)_4Br$ (**5**).

Bond distances (Å)	
Ge(1)–Ge(2)	2.4470(7)
Ge(2)–Ge(3)	2.4548(6)
Ge(3)–Ge(4)	2.4401(7)
Ge(1)–Br(1)	2.3468(8)
Ge(1)–C(1)	1.952(5)
Ge(1)–C(7)	1.944(5)
Ge(2)–C(13)	1.959(5)
Ge(2)–C(19)	1.957(5)
Ge(3)–C(25)	1.964(5)
Ge(3)–C(31)	1.948(5)
Ge(4)–Br(2)	2.3612(8)
Ge(4)–C(37)	1.950(5)
Ge(4)–C(43)	1.952(5)
Bond angles (°)	
Ge(1)–Ge(2)–Ge(3)	115.33(3)
Ge(2)–Ge(3)–Ge(4)	111.25(3)
Br(1)–Ge(1)–Ge(2)	103.36(3)
Br(1)–Ge(1)–C(1)	104.7(2)
C(1)–Ge(1)–Ge(7)	111.6(2)
Br(1)–Ge(1)–C(7)	106.0(2)
C(1)–Ge(1)–Ge(2)	110.6(1)
C(7)–Ge(1)–Ge(2)	119.2(2)
Ge(1)–Ge(2)–C(13)	100.5(1)
Ge(1)–Ge(2)–C(19)	112.9(1)
C(13)–Ge(2)–C(19)	109.4(2)
C(13)–Ge(2)–Ge(3)	110.5(2)
C(19)–Ge(2)–Ge(3)	108.0(2)
Ge(2)–Ge(3)–C(25)	111.2(2)
Ge(2)–Ge(3)–C(31)	111.9(2)
C(25)–Ge(3)–C(31)	108.3(2)
C(25)–Ge(3)–Ge(4)	111.3(1)
C(31)–Ge(3)–Ge(4)	102.6(2)
Ge(3)–Ge(4)–C(37)	118.4(2)
Ge(3)–Ge(4)–C(43)	115.3(1)
Br(2)–Ge(4)–Ge(3)	103.94(3)
Br(2)–Ge(4)–C(37)	104.8(2)
Br(2)–Ge(4)–C(43)	102.8(2)
C(37)–Ge(4)–C(43)	109.6(2)

Fig. 4. Differential pulse voltammogram of $H(GePh_2)_4H$ (**3**, solid line) and $Br(GePh_2)_4Br$ (**5**, dashed line) in CH_2Cl_2 solution using 0.1 mol/L $[Bu^n{}_4N][PF_6]$ as the supporting electrolyte. Conditions used: pulse period = 0.1 s, pulse width = 0.05 s, sample time = 0.02 s.

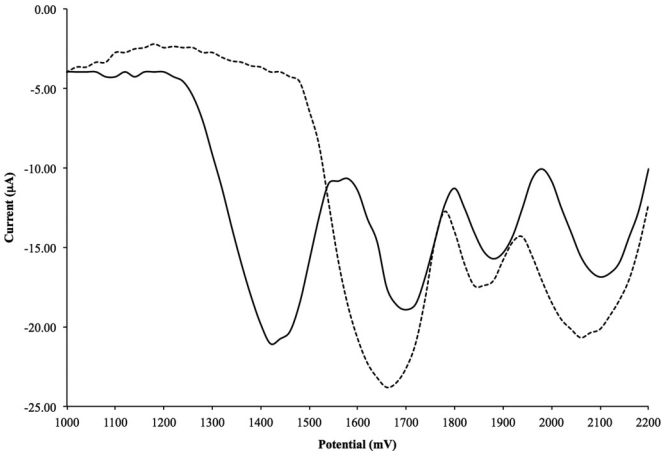

and we have determined that this is due to a trace amount of Br_2 that was present in the sample. However in contrast to all previous investigations, the tetragermane $H(GePh_2)_4H$ (**3**) exhibits four successive oxidation waves in its DPV at 1421, 1772, 1883, and 2101 mV (Fig. 4). The first oxidation of **3** occurs at a less positive potential than that of **5**, and this is expected since **5** contains two electronegative bromine substituents at the termini of the Ge_4 chain. However, the first oxidation of **5** was observed at the same potential as for Ge_4Ph_{10}, suggesting that the highest occupied molecular orbitals of these two species are at approximately the same energy.

The tetragermane **3** was converted to the hexagermane $Pr^i{}_3Ge(GePh_2)_4GePr^i{}_3$ (**1**) via the hydrogermolysis reaction using $Pr^i{}_3GeNMe_2$ in 76% yield (Scheme 3). This reaction proceeds via the in situ conversion of $Pr^i{}_3GeNMe_2$ to the α-germyl nitrile $Pr^i{}_3GeCH_2CN$ by the acetonitrile solvent,[39] where $Pr^i{}_3GeCH_2CN$ is the active species in the germanium–germanium bond forming process. The ^1H NMR spectrum of **1** exhibits a characteristic pattern for the six iso-propyl substituents with a septet at δ 1.48 ppm (J = 7.2 Hz) corresponding to the methine protons and a doublet at δ 0.89 ppm (J = 7.2 Hz) for the methyl groups. The ^{13}C NMR spectrum of **1** contains two resonances at δ 21.2 and 18.2 ppm that are assigned to the germanium-bound carbon atom and the methyl carbon atoms, respectively.

The X-ray crystal structure of **1** was determined, and an ORTEP diagram is shown in Fig. 5, and selected bond distances and angles are collected in Table 4. Compound **1** crystallizes in the *P*–1 space group, and the central Ge–Ge single bond of **1** is located on the inversion center. The germanium–germanium bond distances average 2.4710(3) Å, and the longest of the three crystallographically unique Ge–Ge bond distances is at the central bond. However, the two terminal Ge–Ge bond distances each measure 2.4670(2) and are elongated compared to the typical distance of ca. 2.45 Å due to the presence of three sterically encumbering iso-propyl groups at each atom. Compound **1** is the longest structurally characterized oligogermane to be reported to date, and the length across the Ge_6 chain in **1** measures 12.3515(3) Å.

Each of the germanium atoms in **1** are present in a distorted tetrahedral environment. The average of the two unique Ge-Ge-Ge bond angles is 115.74(1)°, and the more obtuse of the two angles are located at the ends of the molecule, again due to the steric effects of the iso-propyl substituents. The average C-Ge-C bond angle at the terminal germanium atoms is 108.74(7)°, which is close to the idealized tetrahedral angle of 109.5°, while the C-Ge-C bond angles at the internal germanium atoms are slightly more acute, measuring 107.95(6) and 105.92(6)° at Ge(2) and Ge(3), respectively. The nearly tetrahedral environment at the terminal germanium atoms is typical when three relatively large substituents need to be accommodated at a single germanium atom.

The overall geometry of the Ge_6 chain in **1** can be regarded from two different perspectives (Fig. 6). The Ge_6 chain can be considered as being comprised of two sets of three trans-coplanar germanium atoms (Fig. 6*a*), or the four central germanium atoms of **1** can be considered to be mutually coplanar and arranged in a trans-fashion (Fig. 6*b*), with one terminal germanium atom canted above the plane and the other below. In either case, the σ-delocalization present in **1** would carry across all six germanium atoms. However, the second case having four coplanar germanium atoms is similar to the structure of Ge_5Ph_{12}[38] but is extended by one germanium atom, and it is this geometry that can be used to explain the unusual optical and spectral attributes of **1**.

The absorbance maxima for polygermanes $(GeR_2)_n$ fall into the range of approximately 290–340 nm,[22–29,64] and luminescence has been reported for some of these materials as well. The hexagermane **1** has an absorbance maximum (λ_{max}) at 310 nm in its UV–vis spectrum that is red-shifted relative to those for all other reported linear oligogermanes, including Ge_5Ph_{12} and Ge_4Ph_{10} that have λ_{max} values of 295 and 282 nm, respectively. The λ_{max} for **1** falls within the range observed for polygermanes and is similar to the values reported for the alkyl-substituted species $(GeR_2)_n$ (R = Et, λ_{max} = 305 nm; R = Pr^n, λ_{max} = 300 nm; R = Bu^n, λ_{max} = 316 nm).[64] Thus, the degree of σ-delocalization present in **1** is similar to those in the polygermane systems.

The hexagermane **1** is luminescent and exhibits a broad emission band at 370 nm when excited at 312 nm. An overlaid absorbance and emission spectrum of **1** is shown in Fig. 7. Hexagermane **1** is the first discrete oligogermane to exhibit luminescent behavior, and its emission wavelength is nearly identical to that of the polygermane $((Me_3SiOC_6H_4)MeGe)_n$ that was observed at 369 nm.[22] This indicates that oligogermanes might function as useful small-molecule models for the larger polymeric systems. In addition to its luminescence, **1** also interacts with polarized light in dramatic fashion (Fig. 8). When viewed under ambient light, crystals of **1** appear colorless, and when viewed under left-polarized light they appear pale yellow in color. However, when the direction of polarization is reversed, crystals of **1** appear deep blue in color. This phenomenon is due to the packing of **1** in the crystal (Fig. 8), where the four trans-coplanar germanium atoms are stacked in a columnar fashion and the remaining two germanium atoms that are canted above and below the plane are also disposed in a column-like fashion. This imparts long-range chirality for **1** in the solid state, which leads to their observed dichroism.

The DPV of **1** is shown in Fig. 9. The expected pattern of five irreversible oxidation waves was observed with features at 1100, 1383, 1785, 1942, and 2182 mV. The first oxidation wave for **1** was observed at a lower potential than other linear oligogermanes characterized by this method, and this indicates that the σ-bonding HOMO of **1**, which is presumably the source of the first electron that is removed, is destabilized relative to those in other oligogermanes having less than six catenated germanium atoms. We have endeavored to ascertain the reasons that $n - 1$ oxidation waves are observed for these systems. By analogy to photolytic investigations,[64] we postulate that three possible decomposition pathways might be occurring after an oxidation event takes place. A proposed decomposition pathway for **1** after the first oxidation event occurs is shown in Scheme 4. The possible decomposition pathways include germylene extrusion with concomitant chain contraction by one germanium atom, homolytic cleavage of a germanium–germanium single bond to generate two germanium-based radicals, or homolytic Ge–Ge bond cleavage with simultaneous germylene extrusion followed be recombination of the two radical species to generate a new oligogermane. The decomposi-

Scheme 3.

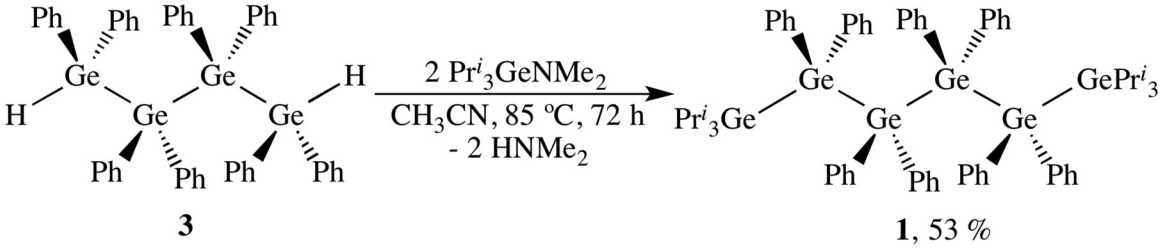

3 **1**, 53 %

Fig. 5. ORTEP diagram of Pr$^i_3$Ge(GePh$_2$)$_4$GePr$^i_3$ (**1**). Thermal ellipsoids are drawn at 50% probability.

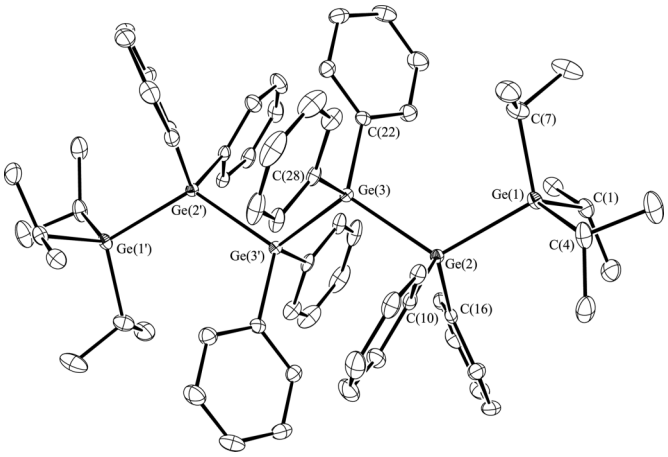

Table 4. Selected bond distances (Å) and angles (°) for Pr$^i_3$Ge(GePh$_2$)$_4$GePr$^i_3$ (**1**).

Bond distances (Å)	
Ge(1)–Ge(2)	2.4670(2)
Ge(2)–Ge(3)	2.4715(3)
Ge(3)–Ge(3′)	2.4745(3)
Ge(1)–C(1)	1.995(2)
Ge(1)–C(4)	1.989(2)
Ge(1)–C(7)	1.995(2)
Ge(2)–C(10)	1.970(2)
Ge(2)–C(16)	1.955(2)
Ge(3)–C(22)	1.967(2)
Ge(3)–C(28)	1.968(2)
Bond angles (°)	
Ge(1)–Ge(2)–Ge(3)	117.330(8)
Ge(2)–Ge(3)–Ge(3′)	114.15(1)
C(1)–Ge(1)–C(4)	108.74(7)
C(1)–Ge(1)–C(7)	108.48(7)
C(4)–Ge(1)–C(7)	108.99(7)
C(1)–Ge(1)–Ge(2)	111.91(4)
C(4)–Ge(1)–Ge(2)	109.19(5)
C(7)–Ge(1)–Ge(2)	109.49(5)
C(10)–Ge(2)–C(16)	107.95(6)
C(10)–Ge(2)–Ge(1)	110.80(4)
C(16)–Ge(2)–Ge(1)	107.71(4)
C(10)–Ge(2)–Ge(3)	100.93(4)
C(16)–Ge(2)–Ge(3)	111.71(4)
C(22)–Ge(3)–C(28)	105.92(6)
C(22)–Ge(3)–Ge(2)	115.68(4)
C(28)–Ge(3)–Ge(2)	99.69(4)
C(22)–Ge(3)–Ge(3′)	108.47(4)
C(28)–Ge(3)–Ge(3′)	112.43(4)

Fig. 6. Structure of the Ge$_6$ skeleton of **1**, viewed as two sets of three coplanar Ge atoms (*a*) or one array of four coplanar Ge atoms (*b*).

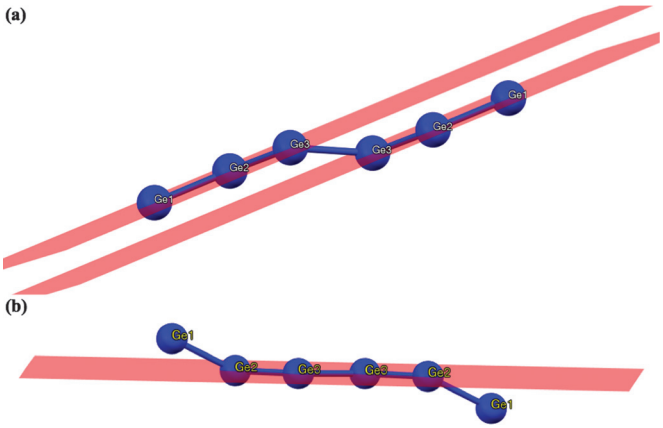

Fig. 7. Absorbance (solid line) and emission spectra (dashed line) of **1** in CH_2Cl_2 solution.

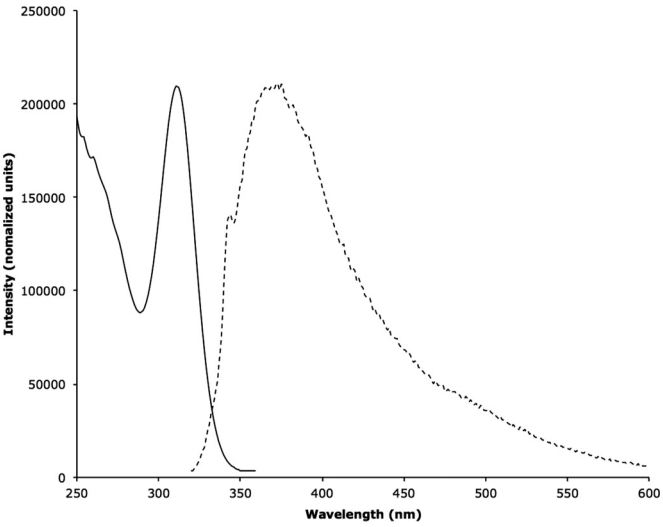

tion products are then oxidized as the sweep continues, and all three sets of possible products shown in Scheme 4 would lead to four additional oxidation events. It is at present unclear which decomposition pathway is occurring for **1**, and we will investigate this in more detail by conducting bulk electrolysis experiments on **1** in the presence of the germylene trapping reagents 2,3-dimethyl-1,3-butadiene (DMB),[65] benzil, acetic acid,[66] and 1,2-diphenylacetlyene,[67] and also will conduct similar studies using lower oligogermanes.

Conclusions

The hexagermane **1** has been prepared and characterized and represents the longest structurally characterized linear oligoger-

Fig. 8. Single crystals of **1** viewed under left-polarized light (*a*) and right-polarized light (*b*) and the crystal packing of **1** viewed along the *b*-axis (*c*).

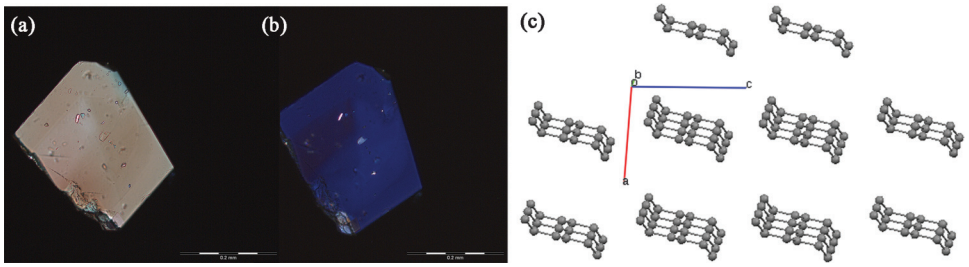

Fig. 9. Differential pulse voltammogram of **1** in CH_2Cl_2 solution using 0.1 mol/L $[Bu^n_4N][PF_6]$ as the supporting electrolyte. Conditions used: pulse period = 0.1 s, pulse width = 0.05 s, sample time = 0.02 s.

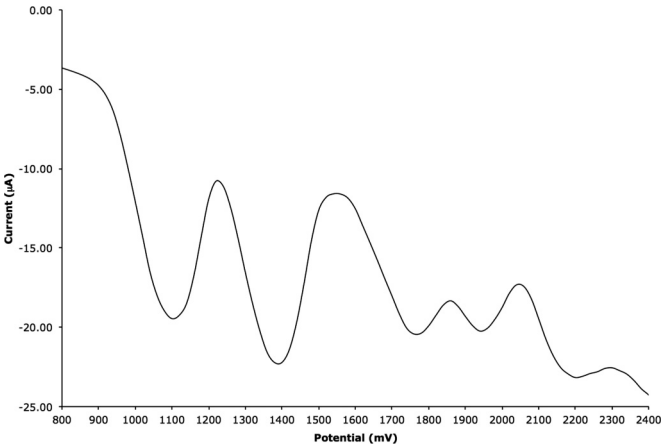

mane to be reported to date. The synthesis of **1** employs the cyclotetragermane **2** as the starting material, and it has been demonstrated that **2** can be synthesized using the hydrogermolysis reaction. Compound **1** is a discrete oligogermane that possesses some of the properties that are known for polygermane systems and is the first such species to exhibit luminescent behavior. Compound **1** also interacts in with different orientations of polarized light, appearing pale yellow under one orientation and deep blue under the other. Thus, **1** serves as a discrete small molecule model for the larger polygermane systems and likely is the first member of a series of long-chain oligogermanes that will possess useful optical and electronic properties.

Experimental section

All manipulations were carried out under a nitrogen atmosphere using standard Schlenk, syringe, and glovebox techniques. Solvents were purified using a Glass Contour solvent purification system. The reagents $ClPh_2GeGePh_2Cl$ (**4**),[42] $HPh_2GeGePh_2H$,[42] $Pr^i_3GeNMe_2$[39] were prepared using literature procedures. The reagents Br_2 and $LiAlH_4$ were purchased from Sigma-Aldrich and used without further purification. ^1H and ^{13}C NMR spectra were recorded at 300 and 75.46 MHz, respectively, using an INOVA Gemini 2000 spectrometer. IR spectra were obtained using a PerkinElmer 1720 infrared spectrometer, and UV–vis spectra were recorded using a Hewlett-Packard 8453 diode array spectrometer. Electrochemical data (CV, DPV, LSV, BE) data were obtained using a DigiIvy DY2312 potentiostat using a glassy carbon working electron, a platinum wire counter electrode, and an Ag/AgCl reference electrode in CH_2Cl_2 solution using 0.1 mol/L $[Bu_4N][PF_6]$ as the supporting electrolyte. Elemental analyses were conducted by Galbraith Laboratories.

Synthesis of $Me_2NPh_2GeGePh_2NMe_2$

To a solution of $ClPh_2GeGePh_2Cl$ (0.546 g, 1.04 mmol) in benzene (20 mL) was added $LiNMe_2$ (0.117 g, 2.29 mmol). The reaction mixture was stirred for 18 h, filtered through Celite, and the solvent was removed from the filtrate in vacuo to yield $Me_2NPh_2GeGePh_2NMe_2$ (0.518 g, 92%) as a pale yellow solid. ^1H NMR (C_6D_6, 25 °C) δ 7.71–7.68 (m, 8H, *o*-H), 7.21–7.18 (m, 12H, *m*-H and *p*-H), 2.78 (s, 12H, –N(CH_3)$_2$) ppm. ^{13}C NMR (C_6D_6, 25 °C) δ 136.3 (*ipso*-C), 135.5 (*o*-C), 129.6 (*p*-C), 128.7 (*m*-C), 42.0 (–N(CH_3)$_2$) ppm. Anal. calcd. for $C_{28}H_{32}Ge_2N_2$: C, 62.05; H, 5.96. Found: C, 61.89; H, 5.88.

Synthesis of $(Ph_2Ge)_4$ (2)

To a solution of $Me_2NPh_2GeGePh_2NMe_2$ (0.461 g, 0.851 mmol) in CH_3CN (170 mL) was added a solution of $HPh_2GeGePh_2H$ (0.388, 0.851 mmol) in CH_3CN (170 mL). The reaction mixture was sealed in a Schlenk tube and was heated at 85 °C for 48 h. The volatiles were removed in vacuo to yield a white solid that was recrystallized from hot toluene to yield **2** (0.602 g, 78%) as colorless crystals. ^1H NMR (C_6D_6, 25 °C) δ 7.56–7.52 (m, 16H, *m*-H), 7.09–6.98 (m, 24H, *o*-H and *p*-H) ppm. ^{13}C NMR (C_6D_6, 25 °C) δ 139.5 (*ipso*-C), 136.5 (*o*-C), 128.5 (*m*-C), 128.7 (*p*-C) ppm. Anal. calcd. for $C_{48}H_{40}Ge_4$: C, 63.52; H, 4.45. Found: C, 63.44; H, 4.48.

Synthesis of $Br(GePh_2)_4Br$ (5)

A suspension of **2** (1.69 g, 1.86 mmol) in benzene (100 mL) was titrated with a 0.059 mol/L solution of bromine in benzene, until the solution remained colorless. The volatiles were removed in vacuo and the resulting solid was washed with Et_2O (3 × 5 mL) and dried in vacuo to yield **3** (1.06 g, 54%) as a white solid. ^1H NMR (C_6D_6, 25 °C) δ 7.60 (d, J = 7.8 Hz, 8 H, *o*-C_6H_5), 7.41 (d, J = 7.5 Hz, 8 H, *o*-C_6H_5), 7.06–6.90 (m, 24 H, *m*-C_6H_5 and *p*-C_6H_5) ppm. ^{13}C NMR (C_6D_6, 25 °C) δ 136.7 (*ipso*-C_6H_5), 134.7 (*ipso*-C_6H_5), 130.0 (*o*-C_6H_5), 129.4 (*o*-C_6H_5), 128.8 (*m*-C_6H_5), 128.6 (*m*-C_6H_5), 128.1 (*p*-C_6H_5), 127.9 (*p*-C_6H_5) ppm. Calcd. for $C_{48}H_{40}Br_2Ge_4$: C, 54.00; H, 3.78. Found: C, 53.87; H, 3.83.

Synthesis of $H(GePh_2)_4H$ (3)

To a solution of **5** (1.20 g, 1.12 mmol) in Et_2O (60 mL) was added $LiAlH_4$ (0.09 g, 2 mmol) under blowing nitrogen. The reaction mixture was stirred for 18 h at room temperature and the volatiles were removed in vacuo. The resulting material was taken up in benzene and filtered through Celite. The benzene was removed in vacuo, and the resulting solid was washed with hexane (3 × 5 mL) and dried in vacuo to yield **3** (1.00 g, 98%) as a white solid. ^1H NMR (C_6D_6, 25 °C) δ 7.50 (d, J = 6.3 Hz, 8 H, *o*-C_6H_5), 7.38 (d, J = 6.3 Hz, 8 H, *o*-C_6H_5), 7.04–6.95 (m, 24 H, *m*-C_6H_5 and *p*-C_6H_5), 5.63 (s, 2H, -Ge-*H*) ppm. ^{13}C NMR (C_6D_6, 25 °C) δ 136.5 (*ipso*-C_6H_5), 136.0 (*ipso*-C_6H_5), 128.9 (*o*-C_6H_5), 128.8 (*o*-C_6H_5), 128.5 (*m*-C_6H_5), 128.3 (*m*-C_6H_5), 128.1 (*p*-C_6H_5), 127.7 (*p*-C_6H_5) ppm. Anal. calcd. for $C_{48}H_{42}Ge_4$: C, 63.37; H, 4.66. Found: C, 63.26; H, 4.59.

Synthesis of $Pr^i_3Ge(GePh_2)_4GePr^i_3$ (1)

To a solution of $Pr^i_3GeNMe_2$ (0.203 g, 0.824 mmol) in CH_3CN (15 mL) was added a solution of **4** (0.43 g, 0.47 mmol) in CH_3CN

Scheme 4.

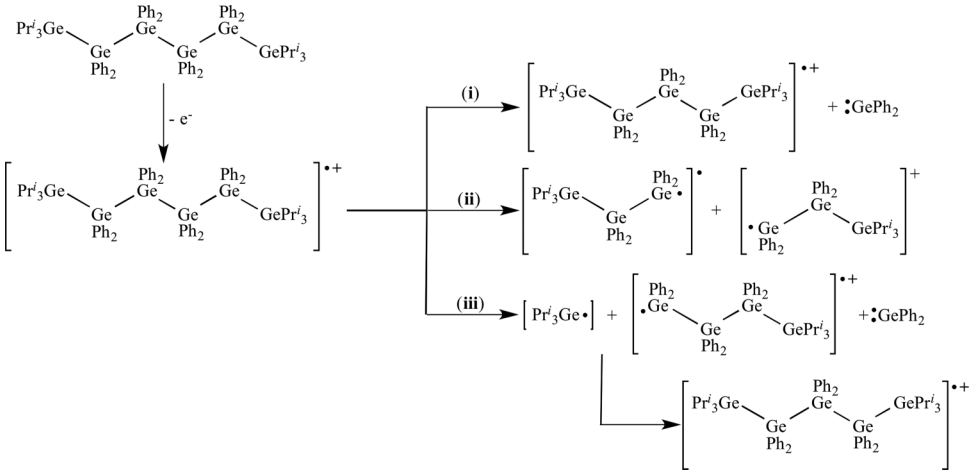

Table 5. Crystallographic data for **1**, **2**, **4**, and **5**.

Compound	**4**	**2**	**5**	**1**
Empirical formula	$C_{24}H_{30}Cl_2Ge_2$	$C_{48}H_{40}Ge_4$	$C_{48}H_{40}Br_2Ge_4$	$C_{66}H_{82}Ge_6$
Formula weight	524.48	907.16	1066.98	1310.86
Temperature (K)	100(2)	150(2)	100(2)	100(2)
Wavelength (Å)	0.71073	0.71073	1.54178	0.71073
Crystal system	Monoclinic	Monoclinic	Monoclinic	Triclinic
Space group	*C*2	$P2_1/c$	$P2_1$	*P*-1
a (Å)	14.947(5)	21.0256(7)	12.8805(2)	11.0685(7)
b (Å)	11.754(4)	10.2387(3)	11.9670(2)	11.3771(6)
c (Å)	13.109(5)	20.4770(7)	13.7534(2)	12.7949(8)
α (°)	90	90	90	97.447(2)
β (°)	108.573(4)	115.583(2)	92.259(1)	91.495(2)
γ (°)	90	90	90	108.292(2)
V (Å^3)	2183(1)	3976.0(2)	2111.04(6)	1513.1(2)
Z, Z′	4, 2	4, 0	2, 0	1, 0
ρ (g·cm^{-1})	1.596	1.515	1.679	1.439
Absorption coefficient (mm^{-1})	3.006	3.028	5.751	2.980
F(000)	1048	1824	1052	670
Crystal size (mm^3)	0.40 × 0.12 × 0.08	0.20 × 0.10 × 0.10	0.27 × 0.24 × 0.22	0.30 × 0.25 × 0.20
θ range for data collection	1.64 to 24.83	1.07 to 26.52°	3.23 to 68.08°	1.91 to 28.36°
Index ranges				
	$-17 \le h \le 17$	$-26 \le h \le 25$	$-15 \le h \le 12$	$-14 \le h \le 12$
	$-13 \le k \le 13$	$-12 \le k \le 11$	$-13 \le k \le 14$	$-11 \le k \le 15$
	$-15 \le l \le 15$	$-25 \le l \le 25$	$-16 \le l \le 16$	$-17 \le l \le 16$
Reflections collected	14 519	28 504	13 170	16 375
Independent reflections	3719 (R_{int} = 0.0906)	8180 (R_{int} = 0.0352)	6320 (R_{int} = 0.0445)	7179 (R_{int} = 0.0221)
Completeness to θ	θ = 24.83 (98.7%)	θ = 25.00 (99.7%)	θ = 66.50 (97.5%)	θ = 25.00 (97.6%)
Absorption correction	Multi-scan	Multi-scan/SADABS	Multi-scan	Multi-scan
Refinement method	Full-matrix least-squares on F^2	Full-matrix least-squares on F^2	Full-matrix least-squares on F^2	Full-matrix least-squares on F^2
Data/restraints/parameters	3719/1/274	8180/0/469	6320/1/488	7179/0/325
Goodness-of-fit on F^2	1.130	1.040	1.019	1.040
Final *R* indices ($I < 2\sigma(I)$)				
R_1	0.0955	0.0327	0.0362	0.0197
wR_2	0.2438	0.0689	0.0890	0.0472
Final *R* indices (all data)				
R_1	0.1017	0.0500	0.0376	0.0244
wR_2	0.2479	0.0741	0.0902	0.0487
Largest diff. peak and hole (e Å^{-3})	1.870 and −0.948	0.889 and −0.669	0.791 and −0.561	0.397 and −0.366

(15 mL). The reaction mixture was sealed in a Schlenk tube and was stirred in an oil bath at 90 °C for 72 h, after which a white precipitate was present. The reaction mixture was cooled and the solid was collected by filtration and washed with hexane (3 × 5 mL) to yield **1** (0.33 g, 53%) as a white solid. ^{1}H NMR (C_6D_6, 25 °C) δ 7.39 (d, *J* = 7.5 Hz, 8 H, *o*-C_6H_5), 7.34 (d, *J* = 7.5 Hz, 8 H, *o*-C_6H_5), 7.15–6.96 (m, 24 H, *m*-C_6H_5 and *p*-C_6H_5), 1.48 (sept, *J* = 7.2 Hz, 6H, –C*H*(CH_3)$_2$), 0.89 (d, *J* = 7.2 Hz, 18 H, –CH(C*H*$_3$)$_2$) ppm. ^{13}C NMR (C_6D_6, 25 °C) δ 137.3 (*ipso*-C_6H_5), 137.0 (*ipso*-C_6H_5), 128.3 (*o*-C_6H_5), 128.2 (*o*-C_6H_5), 128.1 (*m*-C_6H_5), 127.9 (*m*-C_6H_5), 127.7 (*p*-C_6H_5), 127.6 (*p*-C_6H_5), 21.2 (–*C*H(CH_3)$_2$), 18.2 (–CH(*C*H$_3$)$_2$) ppm. Anal. calcd. for $C_{66}H_{82}Ge_6$: C, 60.44; H, 6.31. Found: C, 60.36; H, 6.36.

X-ray crystal structure determinations

Diffraction intensity data were collected with a Siemens P4/CCD diffractometer. Crystallographic data for the X-ray analysis of **1**, **2**, **4**, and **5** are collected in Table 5. The crystal-to-detector distance was 60 mm, and the exposure time was 20 s per frame using a scan width of 0.5°. The data were integrated using the Bruker SAINT software program. Solution by direct methods (SIR-2004) produced a complete heavy atom phasing model consistent with the proposed structures. All non-hydrogen atoms were refined anisotropically by full-matrix least-squares (SHELXL-97). All hydrogen atoms were placed using a riding model. Their positions were constrained relative to their parent atom using the appropriate HFIX command in SHELXL-97.

Supplementary data

Supplementary data are available with the article through the journal Web site at http://nrcresearchpress.com/doi/suppl/10.1139/cjc-2013-0485.

Acknowledgements

Funding for this work was provided by a CAREER grant from the National Science Foundation (No. CHE-0844758) and is gratefully acknowledged.

References

(1) Balaji, V.; Michl, J. *Polyhedron* **1991**, *10*, 1265. doi:10.1016/S0277-5387(00)86103-3.
(2) Miller, R. D.; Michl, J. *Chem. Rev.* **1989**, *89*, 1359. doi:10.1021/cr00096a006.
(3) Corey, J. Y. *Adv. Organomet. Chem.* **2004**, *51*, 1. doi:10.1016/S0065-3055(03)51001-2.
(4) Feigl, A.; Bockholt, A.; Weis, J.; Rieger, B. *Adv. Polym. Sci.* **2010**, *235*, 1. doi:10.1007/12_2009_1.
(5) Jones, R. G.; Holder, S. J. *Polym. Int.* **2006**, *55*, 711. doi:10.1002/pi.1945.
(6) Lambert, J. B.; Pflug, J. L.; Wu, H.; Liu, X. *J. Organomet. Chem.* **2003**, *685*, 113. doi:10.1016/S0022-328X(03)00640-5.
(7) Lukevics, E.; Pudova, O. *Main Group Met. Chem.* **1998**, *21*, 123. doi:10.1515/MGMC.1998.21.3.123.
(8) Marschner, C.; Baumgartner, J.; Wallner, A. *Dalton Trans.* **2006**, 5667. doi:10.1039/b613642g.
(9) Nanjo, M.; Sekiguchi, A. *Adv. Silicon Sci.* **2009**, *2*, 75. doi:10.1007/978-1-4020-8174-3_4.
(10) Krempner, C. *Polymers* **2012**, *4*, 408. doi:10.3390/polym4010408.
(11) Miller, R. D.; Schellenberg, F. M.; Baumert, J. C.; Looser, H.; Shukla, P.; Torruellas, W.; Bjorklund, G. C.; Kano, S.; Takahashi, Y. In *Materials for Nonlinear Optics: Chemical Perspectives (ACS Symposium Series No. 455)*; Marder, S. R., Sohn, J. E., Stucky, G. D., Eds.; American Chemical Society: Washington DC, 1991.
(12) West, R. *J. Organomet. Chem.* **1986**, *300*, 327. doi:10.1016/0022-328X(86)84068-2.
(13) Khan, A.; Gossage, R. A.; Foucher, D. A. *Can. J. Chem.* **2010**, *88* (10), 1046. doi:10.1139/V10-130.
(14) Sita, L. R. *Organometallics* **1992**, *11*, 1442. doi:10.1021/om00040a007.
(15) Sita, L. R. *Acc. Chem. Res.* **1994**, *27*, 191. doi:10.1021/ar00043a002.
(16) Sita, L. R. *Adv. Organomet. Chem.* **1995**, *38*, 189. doi:10.1016/S0065-3055(08)60429-3.
(17) Beckmann, J.; Duthie, A.; Grassmann, M.; Semisch, A. *Organometallics* **2008**, *27*, 1495. doi:10.1021/om8000026.
(18) Choffat, F.; Smith, P.; Caseri, W. *Adv. Mater.* **2008**, *20*, 2225. doi:10.1002/adma.200702268.
(19) Trummer, M.; Choffat, F.; Rami, M.; Smith, P.; Caseri, W. *Phosphorus Sulfur Silicon Relat. Elem.* **2011**, *186*, 1330. doi:10.1080/10426507.2010.543100.
(20) Trummer, M.; Choffat, F.; Smith, P.; Caseri, W. *Macromol. Rapid Commun.* **2012**, *33*, 448. doi:10.1002/marc.201100794.
(21) Trummer, M.; Nauser, T.; Lechner, M.-L.; Uhlig, F.; Caseri, W. *Polym. Degrad. Stab.* **2011**, *96*, 1841. doi:10.1016/j.polymdegradstab.2011.07.012.
(22) Huo, Y.; Berry, D. H. *Chem. Mater.* **2005**, *17*, 157. doi:10.1021/cm0490524.
(23) Katz, S. M.; Reichl, J. A.; Berry, D. H. *J. Am. Chem. Soc.* **1998**, *120*, 9844. doi:10.1021/ja981806q.
(24) Reichl, J. A.; Berry, D. H. *Adv. Organomet. Chem.* **1998**, *43*, 197. doi:10.1016/S0065-3055(08)60671-1.
(25) Reichl, J. A.; Popoff, C. M.; Gallagher, L. A.; Remsen, E. E.; Berry, D. H. *J. Am. Chem. Soc.* **1996**, *118*, 9430. doi:10.1021/ja961777o.
(26) Kashimura, S.; Ishifune, M.; Yamashita, N.; Bu, H.-B.; Takebayashi, M.; Kitajima, S.; Yoshiwara, D.; Kataoka, Y.; Nishida, R.; Kawasaki, S.; Murase, H.; Shono, T. *J. Org. Chem.* **1999**, *64*, 6615. doi:10.1021/jo990180z.
(27) Kobayashi, S.; Cao, S. *Chem. Lett.* **1993**, 1385.
(28) Okano, M.; Takeda, K.; Toriumi, T.; Hamano, H. *Electrochim. Acta* **1998**, *44*, 659. doi:10.1016/S0013-4686(98)00173-X.
(29) Motonaga, M.; Nakashima, H.; Katz, S.; Berry, D. H.; Imase, T.; Kawauchi, S.; Watanabe, J.; Fujiki, M.; Koe, J. R. *J. Organomet. Chem.* **2003**, *685*, 44. doi:10.1016/S0022-328X(03)00236-5.
(30) Amadoruge, M. L.; Weinert, C. S. *Chem. Rev.* **2008**, *108*, 4253. doi:10.1021/cr800197r.
(31) Weinert, C. S. In *Comprehensive Organometallic Chemistry III*; Crabtree, R. H., Mingos, D. M. P., Eds.; Elsevier: London, 2006; Vol. 3, p. 699.
(32) Weinert, C. S. *Dalton Trans.* **2009**, 1691. doi:10.1039/B816067H.
(33) Weinert, C. S. *Comments Inorg. Chem.* **2011**, *32*, 55. doi:10.1080/02603594.2011.618854.
(34) Dräger, M. *Rev. Silicon Germanium Tin Lead Cmpd.* **1983**, *7*, 299.
(35) Okano, M.; Mochida, K. *Chem. Lett.* **1990**, 701. doi:10.1246/cl.1990.701.
(36) Mochida, K.; Hata, R.; Chiba, H.; Seki, S.; Yoshida, Y.; Tagawa, S. *Chem. Lett.* **1998**, 263. doi:10.1246/cl.1998.263.
(37) Roller, S.; Dräger, M. *J. Organomet. Chem.* **1986**, *316*, 57. doi:10.1016/0022-328X(86)82075-7.
(38) Samanamu, C. R.; Amadoruge, M. L.; Schrick, A. C.; Chen, C.; Golen, J. A.; Rheingold, A. L.; Materer, N. F.; Weinert, C. S. *Organometallics* **2012**, *31*, 4374. doi:10.1021/om300385n.
(39) Amadoruge, M. L.; DiPasquale, A. G.; Rheingold, A. L.; Weinert, C. S. *J. Organomet. Chem.* **2008**, *693*, 1771. doi:10.1016/j.jorganchem.2008.01.045.
(40) Amadoruge, M. L.; Gardinier, J. R.; Weinert, C. S. *Organometallics* **2008**, *27*, 3753. doi:10.1021/om800240w.
(41) Amadoruge, M. L.; Golen, J. A.; Rheingold, A. L.; Weinert, C. S. *Organometallics* **2008**, *27*, 1979. doi:10.1021/om800040f.
(42) Amadoruge, M. L.; Short, E. K.; Moore, C.; Rheingold, A. L.; Weinert, C. S. *J. Organomet. Chem.* **2010**, *695*, 1813. doi:10.1016/j.jorganchem.2010.04.015.
(43) Amadoruge, M. L.; Yoder, C. H.; Conneywerdy, J. H.; Heroux, K.; Rheingold, A. L.; Weinert, C. S. *Organometallics* **2009**, *28*, 3067. doi:10.1021/om900035r.
(44) Samanamu, C. R.; Amadoruge, M. L.; Weinert, C. S.; Golen, J. A.; Rheingold, A. L. *Phosphorus Sulfur Silicon Relat. Elem.* **2011**, *186*, 1389. doi:10.1080/10426507.2010.543114.
(45) Samanamu, C. R.; Amadoruge, M. L.; Yoder, C. H.; Golen, J. A.; Moore, C. E.; Rheingold, A. L.; Materer, N. F.; Weinert, C. S. *Organometallics* **2011**, *30*, 1046. doi:10.1021/om101091c.
(46) Samanamu, C. R.; Materer, N. F.; Weinert, C. S. *J. Organomet. Chem.* **2012**, *698*, 62. doi:10.1016/j.jorganchem.2011.10.026.
(47) Subashi, E.; Rheingold, A. L.; Weinert, C. S. *Organometallics* **2006**, *25*, 3211. doi:10.1021/om060115x.
(48) Schrick, A. C.; Weinert, C. S. *Mater. Res. Bull.* **2013**, *48*, 4390. doi:10.1016/j.materresbull.2013.05.113.
(49) Schrick, E. K.; Forget, T. J.; Roewe, K. D.; Schrick, A. C.; Moore, C. E.; Golen, J. A.; Rheingold, A. L.; Materer, N. F.; Weinert, C. S. *Organometallics* **2013**, *32*, 2245. doi:10.1021/om400132z.
(50) Samanamu, C. R.; Rheingold, A. L.; Weinert, C. S. *J. Organomet. Chem.* **2011**, *696*, 3721. doi:10.1016/j.jorganchem.2011.08.029.
(51) Weinert, C. S. *ISRN Spectrosc.* **2012**, Article ID 718050. doi:10.5402/2012/718050.
(52) Roewe, K. D.; Rheingold, A. L.; Weinert, C. S. *Chem. Commun.* **2013**, *49*, 8380. doi:10.1039/c3cc45450a.
(53) Ritter, S. K. *Chem. Eng. News* **2013**, *91*, 6.
(54) Ross, L.; Dräger, M. *J. Organomet. Chem.* **1980**, *199*, 195. doi:10.1016/S0022-328X(00)83852-8.
(55) Simon, D.; Häberle, K.; Dräger, M. *J. Organomet. Chem.* **1984**, *267*, 133. doi:10.1016/0022-328X(84)80168-0.
(56) Dräger, M.; Ross, L. *Z. Anorg. Allg. Chem.* **1980**, *469*, 115. doi:10.1002/zaac.19804690117.
(57) Rupar, P. A.; Jennings, M. C.; Baines, K. M. *Organometallics* **2008**, *27*, 5043. doi:10.1021/om800368d.
(58) Sekiguchi, A.; Yatabe, T.; Naito, H.; Kabuto, C.; Sakurai, H. *Chem. Lett.* **1992**, 1697. doi:10.1246/cl.1992.1697.
(59) Mochida, K.; Kawajiri, Y.; Goto, M. *Bull. Chem. Soc. Jpn.* **1993**, *66*, 2773. doi:10.1246/bcsj.66.2773.
(60) Dräger, M.; Simon, D. *Z. Anorg. Allg. Chem.* **1981**, *472*, 120. doi:10.1002/zaac.19814720114.
(61) Roller, S.; Simon, D.; Dräger, M. *J. Organomet. Chem.* **1986**, *301*, 27. doi:10.1016/0022-328X(86)82053-8.
(62) Häberle, K.; Dräger, M. *J. Organomet. Chem.* **1986**, *312*, 155. doi:10.1016/0022-328X(86)80294-7.
(63) Mochida, K.; Hodota, C.; Hata, R.; Fukuzumi, S. *Organometallics* **1993**, *12*, 586. doi:10.1021/om00026a052.
(64) Mochida, K.; Chiba, H. *J. Organomet. Chem.* **1994**, *373*, 45. doi:10.1016/0022-328X(94)80104-5.
(65) Leigh, W. J.; Toltl, N. P.; Apodaca, P.; Castruita, M.; Pannell, K. H. *Organometallics* **2000**, *19*, 3232. doi:10.1021/om000174p.
(66) Huck, L. A.; Leigh, W. J. *Organometallics* **2007**, *26*, 1339. doi:10.1021/om0609362.
(67) Harrington, C. R.; Leigh, W. J.; Chan, B. K.; Gaspar, P. P.; Zhou, D. *Can. J. Chem.* **2005**, *83* (9), 1324. doi:10.1139/v05-148.